

Electronic Supplementary information

Geometric design of micron-sized crystalline silicon anodes from in situ

observing deformation and fracture behaviors[†]

Xing-yu Zhang,^a Wei-Li Song,^b Zhan-li Liu,^c Hao-sen Chen,^{*b} Teng Li,^d Yu-jie Wei^e and Dai-ning Fang^{*ab}

^aState Key Laboratory for Turbulence and Complex Systems, College of Engineering, Peking University, Beijing, 100871, China. Email: fangdn@pku.edu.cn; Tel: +86-010-62753795

^bState Key Laboratory of Explosion Science and Technology, Institute of Advanced Structure Technology, Beijing Institute of Technology, Beijing 100081, China. Email: chenhs@bit.edu.cn; Tel: +86-010-68913302

^cApplied Mechanics Laboratory, School of Aerospace Engineering, Tsinghua University, Beijing 100084, China

^dDepartment of Mechanical Engineering, University of Maryland, College Park, Maryland 20742, USA

^eLMN, Institute of Mechanics, Chinese Academy of Sciences, Beijing 100190, China

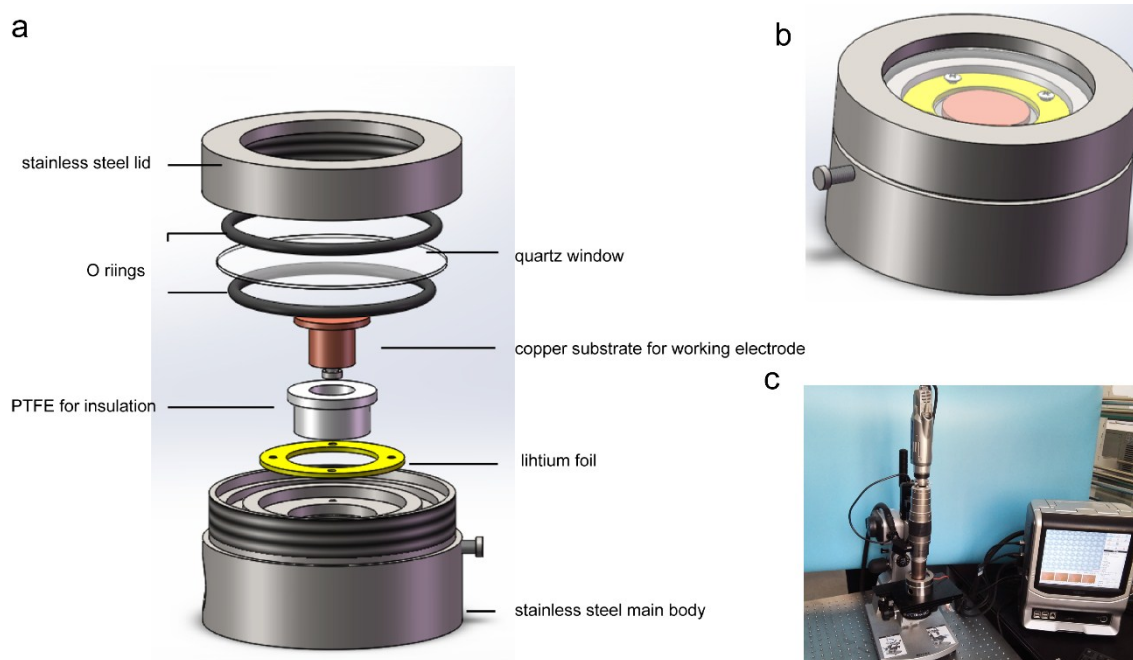


Fig. S1. (a) schematic of each component of the home-made battery cell. The quartz window allows optical access to the silicon micropillars during the electrochemical operation. Two O-rings are used to seal the cell. The polytetrafluoroethylene (PTFE) substrate is to insulate the stainless steel main body and the copper substrate. The lithium foil and the working electrode are arranged side by side, which makes the cell no polymer separator and leads to inhomogeneous lithium flux that lets some of $\{1\ 1\ 0\}$ crystal planes fracture earlier than other $\{1\ 1\ 0\}$ planes. (b) Assembly of the custom battery cell. (c) Photography of the in-situ optical observation platform used for electrochemical testing.

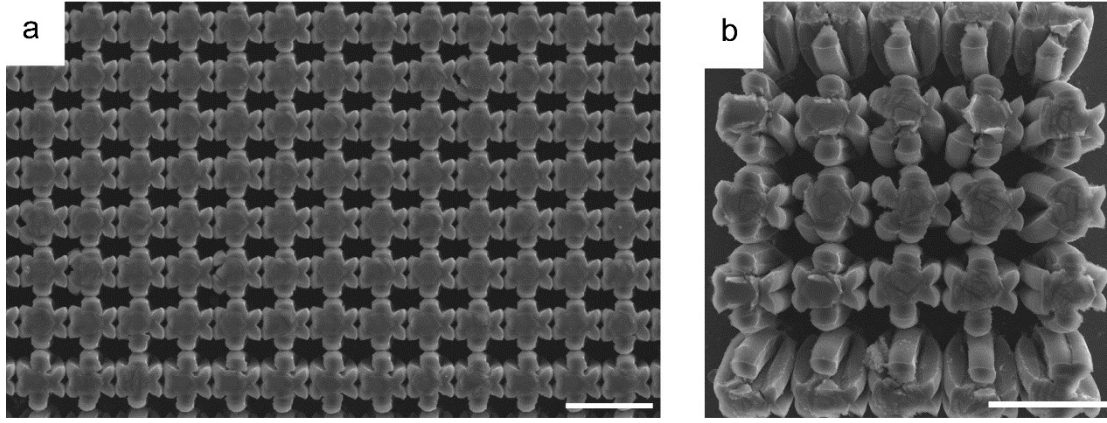


Fig. S2. SEM images of single-crystalline silicon micropillars with solid structures after lithiation for several hours, which demonstrated (a) the homogeneity of the deformation and (b) reasonability of surface information reflecting the entire micropillar. Galvanostatic discharge (lithiation) current density is $450 \mu\text{Acm}^{-2}$ above 0.1V, and then galvanostatic discharge is set to be $150 \mu\text{Acm}^{-2}$ for 8 hours. Here, the scale bars are 50 μm .

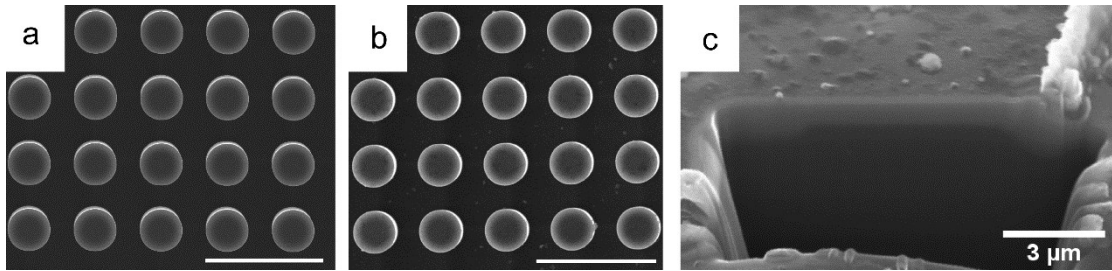


Fig. S3. SEM images of single-crystalline silicon micropillars with solid structures (a) before lithiation and (b) after lithiation with 0.12 V cut-off voltage. No deformation was observed at this cut-off voltage. (c) FIB cutting image of silicon substrate after galvanostatic discharging. The relative depth of lithiation (RDOL), defined as $\text{RDOL} = (\text{Capacity}_t - \text{Capacity}_{U=0.12\text{V}}) / \text{Capacity}_{\text{theory}}$, excluded the capacity of silicon substrate during the computation of theoretical capacity ($\text{Capacity}_{\text{theory}}$) due to small proportion at first lithiation, where Capacity_t is the capacity at the concerned time, and $\text{Capacity}_{U=0.12\text{V}}$ is the capacity at $U=0.12\text{V}$. Galvanostatic discharge (lithiation) current density is $450 \mu\text{Acm}^{-2}$ above 0.1V, and then galvanostatic discharge is adjusted to be $150 \mu\text{Acm}^{-2}$ for 8 hours. The scale bars are 50 μm in Fig. S3a, b.

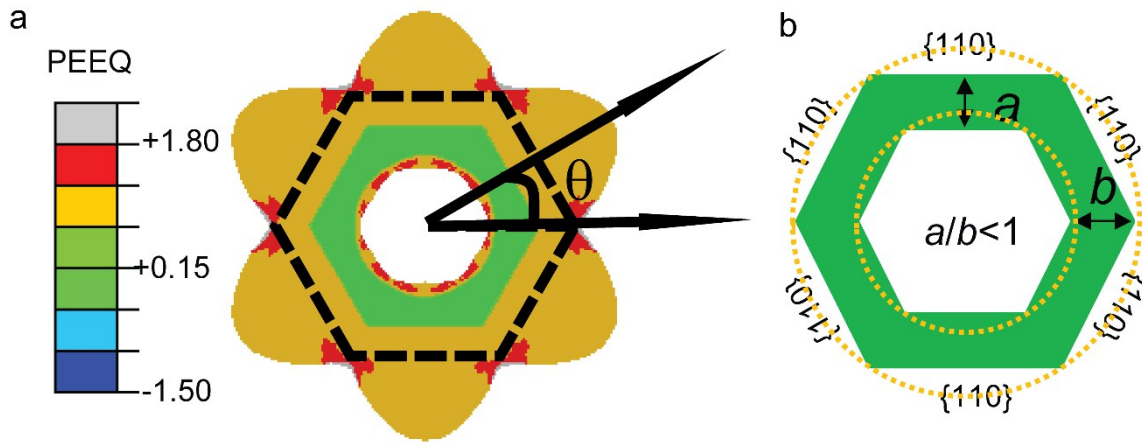


Fig. S4. (a) strain concentration at $\theta=0^\circ, 60^\circ, 120^\circ, 180^\circ, 240^\circ$ and 320° due to anisotropic deformation along different crystallographic orientation, which leads to fracture. This fracture mechanism inspires a design strategy that gives the slowing moving orientation larger dimensions. This strategy can circumvent the anisotropy to be a more uniform volume changes, which leads to alleviate the strain concentration.^[1] (b) top-view schematic of a anisometric hexagonal prism. The thickness b along the fast moving direction (e.g. $\theta=0^\circ$) is set to be larger than the thickness a along the slow moving direction (e.g. $\theta=90^\circ$), which meets the feature of the anisometric structure ($a/b=\sqrt{3}/2$).

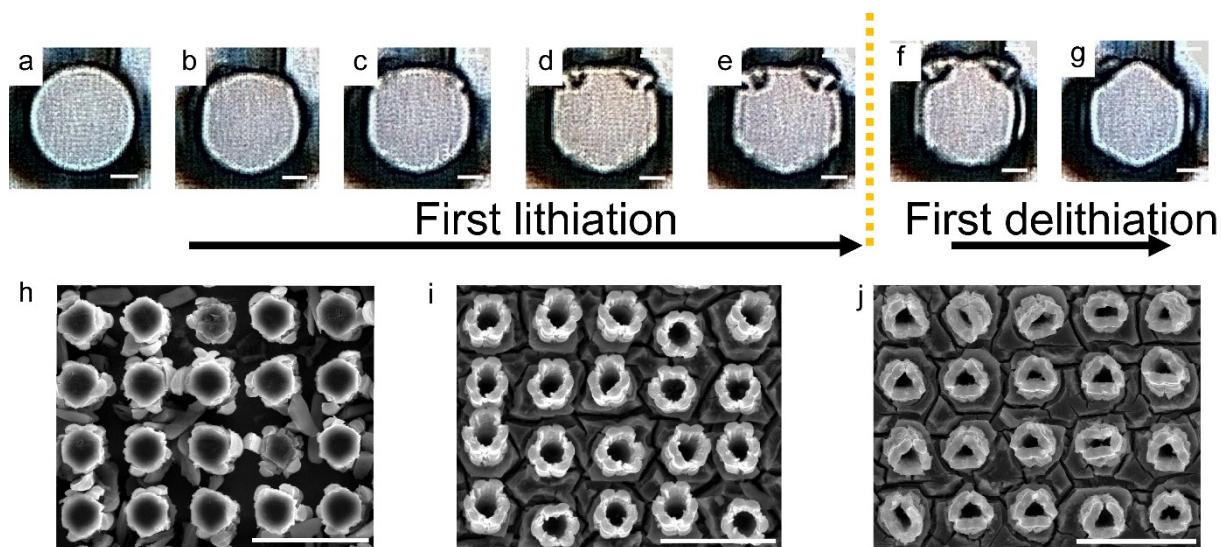


Fig. S5. The optical images of morphological evolution: (a) initial configuration before lithiation. (b) Volume expansion. (c) Crack initiation. (d) Crack penetration. (e) Crack deflection and interface delamination at the a-Si/c-Si interface during initial lithiation. (f) Detachment of a-Si from c-Si micropillars. (g) The hexagonal c-Si solely remained on the substrate. The SEM images of morphological changes of (h) solid structures, (i) isometric hollow structures and (j) anisometric structures after three discharging/charging cycles at $150 \mu\text{Acm}^{-2}$. A larger proportion of the lithium-silicide detached from the solid micropillars during delithiation, which remained residual fresh c-Si that again was inserted by lithium next lithiation. The kinetic process lead to more loss of capacity and lower Coulombic efficiency. In contrary, the hollow structures maintained better mechanical integrity, though the silicon substrate suffered fracture due to over-charging (lithiation). In addition, the reversibility of deformation was also observed by in-situ optical method, which was the main reason of greater Coulombic efficiency. Here, the scale bars are $5\mu\text{m}$ (a-g) and $50\mu\text{m}$ (h-j).

Supplementary Notes

Note S1: Finite element modeling of lithiation under unclamped micropillars

The finite element method (FEM) is used to simulate the anisotropic deformation and stress analysis by ABAQUS/Standard (6.13 version) to understand crack initiation and seek a strategy to alleviate fracture behavior. The plane strain condition was assumed due to experimental observation of slight variation of height in the axial direction and larger size of height than the in-plane dimensions. The difference of elastic properties along different crystalline orientations was neglected to assume that the crystalline silicon (c-Si) is an isotropic perfectly elastic-plastic material with an elastic modulus E of 185GPa, a Poisson's ratio ν of 0.28 and a yield strength Y of 7GPa. The lithiated silicon (amorphous silicon, a-Si, or lithium-silicide) was assumed to be an isotropic elastic and perfectly plastic material ($E=35$ GPa, $\nu=0.22$ and $Y=1.5$ GPa) of which the Cowper-Symonds overstress power law with proper parameters was applied to approximate the perfectly plastic limit.^[2] Due to two-phase diffusion and the analogy between the volume expansion of lithium concentration and the thermal expansion of temperature field, specifying a sharp moving temperature field is modeled as the sharp interface of c-Si and a-Si moving towards to the core of solid electrodes. The lithiation expansion coefficient is set to be 0.4 to simulate about a 300% volume expansion.^[3]

In addition, the isometric hollow structures with thickness-radius ratios $t/R=0.70$ and 0.45 are also simulated by the above mentioned FEM (Fig. 5c,d). The difference with solid structures is that lithium can also insert the inner surface. Due to the slower inserted rate at the inner surface than that of the outside surface (experimental observation in Fig. 4a of the main body in this work), the marching speed of the moving temperature field from the outside surface is 12.5 times faster than the maximum marching speed from the inner surface by which the deformation simulated is in agreement with the experimental observation. It is important to

note that the insertion lithiation at the inner surface is neglected for $t/R=0.3$ and 0.35 in the simulation in Fig. 6b due to requirement of convergence, which has few effect on the tendency of CAF (capability to alleviate fracture).

Supplementary References:

- [1] Y. An, B. C. Wood, J. Ye, Y. Chiang, Y. M. Wang, M. Tang, H. Jiang, *PHYS CHEM CHEM PHYS* 2015, 17, 17718.
- [2] H. Yang, F. Fan, W. Liang, X. Guo, T. Zhu, S. Zhang, *J MECH PHYS SOLIDS* 2014, 70, 349.
- [3] I. Ryu, S. W. Lee, H. Gao, Y. Cui, W. D. Nix, *J POWER SOURCES* 2014, 255, 274